

# Membrane Curvature, Lipid Segregation, and Structural Transitions for Phospholipids under Dual-Solvent Stress<sup>†</sup>

R. P. Rand\* and N. L. Fuller

*Biological Sciences, Brock University, St. Catharines, Ontario, L2S 3A1 Canada*

S. M. Gruner

*Physics Department, Princeton University, Princeton, New Jersey 08544*

V. A. Parsegian

*National Institutes of Health, Bethesda, Maryland 20892*

*Received May 15, 1989; Revised Manuscript Received July 25, 1989*

**ABSTRACT:** Amphiphiles respond both to polar and to nonpolar solvents. In this paper X-ray diffraction and osmotic stress have been used to examine the phase behavior, the structural dimensions, and the work of deforming the monolayer-lined aqueous cavities formed by mixtures of dioleoylphosphatidylethanolamine (DOPE) and dioleoylphosphatidylcholine (DOPC) as a function of the concentration of two solvents, water and tetradecane (td). In the absence of td, most PE/PC mixtures show only lamellar phases in excess water; all of these become single reverse hexagonal ( $H_{II}$ ) phases with addition of excess td. The spontaneous radius of curvature  $R_0$  of lipid monolayers, as expressed in these  $H_{II}$  phases, is allowed by the relief of hydrocarbon chain stress by td;  $R_0$  increases with the ratio DOPC/DOPE. Mixtures with very large  $R_0$ 's can have water contents higher than the  $L_\alpha$  phases that form in the absence of td. The drive for hydration is understood in terms of the curvature energy to create large water cavities in addition to direct hydration of the polar groups. Much of the work of removing water to create hexagonal phases of radius  $R < R_0$  goes into changing monolayer curvature rather than dehydrating polar groups. Single  $H_{II}$  phases stressed by limited water or td show several responses. (a) The molecular area is compressed at the polar end of the molecule and expanded at the hydrocarbon ends. (b) For circularly symmetrical water cylinders, the degrees of hydrocarbon chain splaying and polar group compression are different for molecules aligned in different directions around the water cylinder. (c) A pivotal position exists along the length of the phospholipid molecule where little area change occurs as the monolayer is bent to increasing curvatures. (d) By defining  $R_0$  at the pivotal position, we find that measured energies are well fit by a quadratic bending energy,  $K_0/2 (1/R - 1/R_0)$ ; the fit yields bilayer bending moduli of  $K_c = (1.2 - 1.7) \times 10^{-12}$  ergs, in good agreement with measurements from bilayer mechanics. (e) For lipid mixtures, enforced deviation of the  $H_{II}$  monolayer from  $R_0$  is sufficiently powerful to cause demixing of the phospholipids in a way suggesting that the DOPE/DOPC ratio self-adjusts so that its  $R_0$  matches the amount of td or water available, i.e., that curvature energy is minimized.

**A**mphiphiles by their very nature respond both to polar and to nonpolar solvents. The vast literature on micelles, emulsions, and microemulsions testifies to the rich variety of structures that result from the simultaneous expression of dual polar and nonpolar tendencies. Phospholipids, generally expected to form bilayer structures reminiscent of those found in cell membranes, have been clearly shown by Reiss-Husson and Luzzati (1962) to form nonbilayer structures in a variety of aqueous conditions. This seminal work launched many studies on the rich polymorphism of these lipids in aqueous environments [for an early review, see Luzzati (1968)].

For some time it has been known that one very common nonbilayer structure that many phospholipids will take on is an inverted hexagonal structure of parallel cylinders of water bounded by lipid polar groups with the space between the cylinders filled by nonpolar components. An enormous literature now exists of studies examining the role of temperature, polar group and hydrogen chain species, non-phospholipid molecules, and water content in the bilayer-hexagonal

structural transition [for a recent review, see Gruner et al. (1985)]. This has made it possible to see the balance of structural tendencies in these lipids and to understand how shifting that balance creates phase transitions or phase separations. This has usually been explained in terms of molecular shape or excluded volume.

Although there exists an extensive literature on surfactant-water-oil phase behavior [e.g., see Bellocq (1987)], it is surprising that phospholipids have not been more widely studied for the many structures they can form when exposed to nonpolar solvents. Only relatively recently however has it been recognized that the formation of nonbilayer structures can be stimulated by addition of alkane (Kirk & Gruner 1985). Significantly, Tate and Gruner (1987) have shown that small quantities of lipids, which would normally stabilize the bilayer, if endowed with particularly long hydrocarbon chains can also induce the hexagonal transition. This suggests that such unusual lipids may play the role of solvent in solvent-free membranes. With such information, one now sees new tendencies to form nonbilayer structures. Gruner and co-workers have utilized the idea of a spontaneous (also called "intrinsic" or "equilibrium") monolayer curvature,  $1/R_0$ , for each phospholipid or mixture of phospholipids, akin to the ideas originally developed by Helfrich (1973) for bilayers. It has been

<sup>†</sup> R.P.R. acknowledges the financial support of the Natural Sciences and Engineering Research Council of Canada. S.M.G. was supported by NIH Grant GM 32614 and DOE Grant DE-FG02-87ER60522-A000.

shown that near full hydration the work of changing the curvature of an  $H_{II}$  monolayer can be approximated by a quadratic function of the difference between actual and spontaneous radii of curvature (Gruner et al., 1986). The spontaneous curvature is used to explain the tendency to form nonbilayer structures, a tendency that is allowed when there is sufficient nonpolar solvent or freedom of motion in the hydrocarbon chains. Frustration, by deprivation of such molecules that affect the aliphatic regions, can be an important energetic factor in bilayer formation. It has been argued that such stress is an unrecognized factor in the normal activity of lipids in functioning membranes (Gruner, 1985, 1989).

Our purpose here is to examine the effects of stressing such systems not only in the polar group region by restricting water but also in the hydrocarbon region by limiting the nonpolar solvent. The phospholipid hydrocarbon chains are intentionally kept the same to examine the qualitative differences wrought by changes in the polar groups. Alone, in excess water at room temperature, dioleoylphosphatidylethanolamine (DOPE) forms a hexagonal phase while dioleoylphosphatidylcholine (DOPC) takes on a lamellar form. Their mixtures in water, given sufficient DOPC, are dominated by lamellar phases. But gradual addition of alkane stimulates the gradual increase in amount of a coexisting hexagonal phase. Its  $R_0$  can be increased by increasing the DOPC/DOPE ratio, apparently reflecting DOPC's larger polar group size or degree of hydration. The effects of different concentrations of alkane and water, of different ratios of lipids, and of removing water solvent from the different structures all bring out features of lipid packing that would be unrecognized if one were confined to studying lipid/water mixtures in the absence of nonpolar solvents.

The dual-solvent affinity of an amphiphile is not a simple matter of two parts of a single molecule seeking two kinds of solvent. Each affects the other. Addition of an alkane to a phospholipid creates a hexagonal structure whose curvature requires more water than did the antecedent lamellar phase. But a lamellar phase of the same lipids in limited water holds on to water much more tenaciously than does the hexagonal form at the same level of hydration. It is the interplay of such solvation phenomena that is the subject of this work.

In these studies we used X-ray diffraction to measure dimensions of the lipid structures. The osmotic stress method (Parsegian et al., 1986), originally developed to measure forces between bilayers in multilayer arrays, was used to measure the work of deforming the aqueous cavities in the hexagonal phase. It has become possible to map the phase diagram and structural dimensions of a lipid/water system at the same time as one determines the free energy of the components in the lipid phase. Thus, thermodynamic and structural information are brought together to study structure in terms of its causative energies. Two remarkable features emerge as one bends lipid monolayers, enforcing deviations from  $R_0$ . First, there is a neutral or pivotal position along the length of the phospholipid molecule, each side of which molecular areas change in opposite directions as the monolayer is bent. That position can nicely define where, in the lipid molecules, the lateral intermolecular forces may balance. Second, lipids in mixed systems tend to segregate, apparently adjusting their composition to simultaneously minimize bending and hydrocarbon packing energies.

#### MATERIALS AND METHODS

DOPE and DOPC were obtained from Avanti Polar Lipids (Birmingham, AL) and checked for purity by thin-layer chromatography before and, occasionally, after the experi-

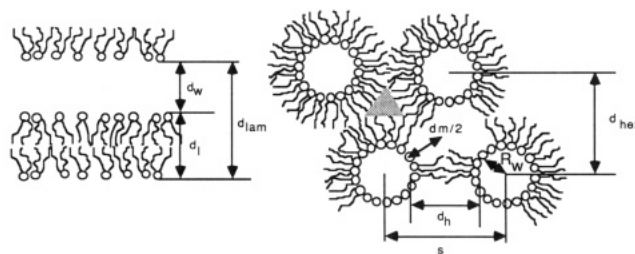


FIGURE 1: Structural parameters describing the hexagonal and lamellar phases derived from X-ray, compositional, and density data as described in the text.  $\phi_1$  is the volume fraction of the nonaqueous portion of the sample, and  $V_1$  is the volume of one phospholipid molecule. For the lamellar phase,  $d_l = \phi_1 d_{lam}$ ,  $d_w = d_{lam} - d_l$ , and  $A = 2V_1/d_l$ . For the hexagonal phase,  $s = 2d_{hex}/\sqrt{3}$ ,  $R_w^2 = [2d_{hex}^2(1 - \phi_1)]/(\pi\sqrt{3})$ ,  $d_h = s - 2R_w$ ,  $d_m = 2(s/\sqrt{3} - R_w)$ , and  $A(r) = \sqrt{3}\pi r V_1/(d_{hex}^2 \phi_1)$  = area occupied by one lipid molecule of volume  $V_1$  on the surface of a cylinder of radius  $r$ .

ments. The lipids were stored under nitrogen at  $-18^\circ\text{C}$  until used. Lipid mixtures were produced by combining the appropriate amounts of the component lipids in organic solvent and then removing the solvent under vacuum. The lipid was hydrated either by weighing the dry lipid and 2 mM TES buffer (pH 7.3) into small weighing bottles, and equilibrating in the dark, at room temperature, for 48 h, or by equilibrating with polyethylene glycol solutions of measured osmotic pressure or with vapors of saturated salt solutions of known vapor pressure (Parsegian et al., 1986). No water loss was detected before the hydrated lipid was mounted into X-ray sample holders at the equilibrating temperature. Each sample was combined with some powdered Teflon (as an X-ray calibration standard) and sealed between mica windows 1 mm apart. X-ray diffraction was used to characterize the structures formed by the various lipid mixtures. The Cu  $K\alpha_1$  line ( $\lambda = 1.540 \text{ \AA}$ ) was isolated with a bent quartz crystal monochromator, and diffraction patterns were recorded photographically with Guinier X-ray cameras operating in vacuo.

All samples formed lamellar or hexagonal phases. A lamellar phase is characterized by a series of three to five X-ray spacings in the ratios of the unit-cell dimensions,  $d_{lam}$ : 1, 1/2, 1/3, 1/4, etc. A hexagonal phase is characterized by X-ray spacings bearing ratios to the dimension of the first order,  $d_{hex}$ , of 1,  $1/\sqrt{3}$ ,  $1/\sqrt{4}$ ,  $1/\sqrt{7}$ ,  $1/\sqrt{9}$ ,  $1/\sqrt{11}$ , etc. Many samples showed two populations of X-ray spacings of the lamellar and hexagonal series, indicating the coexistence of two phases. Their relative abundance can be judged approximately by the relative intensity of each population of X-ray reflections. Note that the lattice dimensions ( $\pm 0.1 \text{ \AA}$ ) are so dependent on the PE/PC ratio (see Figure 2) that it is experimentally difficult to prepare separate PC/PE mixtures to the same ratio as assayed by X-ray diffraction. Depending on the sample composition, the time lag before the appearance of a second phase, indicating lipid segregation, varied from hours to days (see Results). All experiments were performed at approximately  $22^\circ\text{C}$ .

For a single hexagonal or lamellar phase of known composition, the unit cell can be divided into lipid and aqueous compartments as shown in Figure 1, each containing all of the lipid or all of the water. This volume-average division follows the method originally introduced by Luzzati and Husson (1962). The dimensions derived in that division, as described in the equations of Figure 1, depend on the densities of the various components and the assumption of linear addition of the bulk specific volumes of the components. The global specific volumes of many phospholipids have been measured directly; that of the hydrocarbon chains of the lipids was

derived as  $1.17 \text{ cm}^3/\text{g}$  [see Rand and Paresgian (1989) for a detailed discussion of molecular densities].

The molecular area  $A$ , bilayer thickness  $d_b$ , and bilayer separation  $d_w$  for lamellar phases are given by the formulas of Figure 1. For hexagonal phases it has been assumed that the water cores are cylindrical in cross section, an assumption shown to be valid in the case of DOPE phases in excess water (Turner & Gruner 1989). Then,  $s$  is the interaxial distance between cylinders,  $R_w$  is the radius of the water cylinder, and  $d_h$  is the intercylinder lipid thickness;  $d_m$  is twice the distance, nominally two molecular lengths, from the cylinder surface to the hexagonal interstice (the center of the shaded area in Figure 1). In the hexagonal structure the estimated molecular area depends on the position along the molecule in the hexagonal structure. It is calculated at  $R_w$ , the lipid-water interface, as  $A_w$ , at a "pivotal" position along the molecule (described in the Results) as  $A_{pp}$ , and at the "terminal" distance,  $A_t$ , taken to be halfway along the interaxial line between cylinders. The lipid polar groups are defined as including all polar moieties including the carbonyls at the ends of the attached fatty acid hydrocarbon chains (Rand & Parsegian, 1989). The amount of tetradecane (td) added to these mixtures *always* refers to its weight percent of the total lipid (nonaqueous) weight. The shaded area in Figure 1 represents an interstice whose volume must be filled with hydrocarbon chains or alkane. From the hexagonal geometry, the volume of the interstices is taken as that volume left after subtracting the volume occupied by the maximum-sized circular cylinders of radius  $s/2$  from the unit-cell volume. It is 0.0931 of the unit-cell volume. The formulas of Figure 1 apply to single phases. It can be difficult to determine if added tetradecane is fully incorporated into the lipid or if some of it coexists as a separate phase. As with water uptake, we assume that td uptake occurs over the concentration range for which the lipid lattice spacing changes with tetradecane concentration.

Samples in which the water stress was measured, by either the osmotic or vapor pressure methods, were X-rayed to determine the hexagonal lattice spacing. Their composition and structural parameters were then derived by referring to the equivalent dimension of the gravimetrically prepared samples. A model-independent presentation of the data is given by the relation between the osmotic pressure, or negative hydrostatic pressure within the water cylinders, and the water volume per lipid molecule. Structural dimensions within the hexagonal phase, modeled according to the volume-averaged regions as described above, allow these data to be translated in ways that show how the structure depends on the water and hydrocarbon stresses.

## RESULTS

We present the data under four regimes of solvent stress in the following order: (a) no stress, the lipid assembles into whatever structure it will in the presence of both excess water and excess td; (b) water stress but no td stress, the lipid assembles in limited amounts of water, where td appears to be in excess; (c) td stress but no water stress, the lipid, with limited amounts of td, assembles in excess water; (d) both td and water stress, the lipid assembles under conditions in which both water and td are limited in a controlled way.

(a) *No Stress*. What dimensions does the hexagonal phase take on without the stress of being deprived of either water or added alkane, i.e., where each is in excess? Figure 2 and Table I show the structural parameters of hexagonal phases formed by various DOPE/DOPC mixtures in excess of both water and tetradecane. The addition of PE to PC, which alone forms a lamellar structure, creates hexagonal lattices of de-

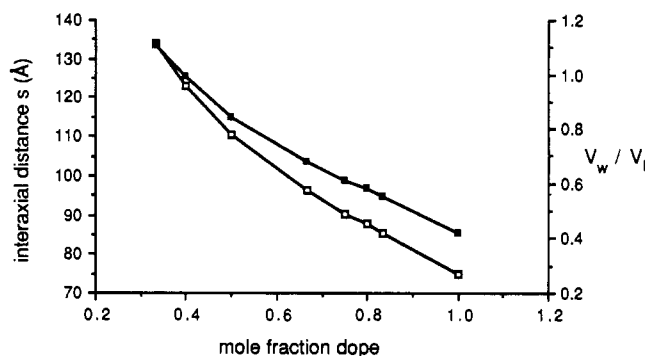


FIGURE 2: A plot of interaxial distance  $s$  (open symbols) and the ratio of the water/lipid volumes (closed symbols) in the maximally hydrated hexagonal phases formed in excess water and tetradecane by various DOPE/DOPC mole ratios. The corresponding radii of the water cylinders varies from 21 to 42 Å (Table I).

Table I: Structural Dimensions of DOPE/DOPC Hexagonal Phases Formed in Excess Water and Tetradecane

mol % PE	DOPE/ DOPC mole ratio	$d_{\text{hex}}$ (Å)	$s$ (Å)	$V_w/V_l$	$R_w$ (Å)
1.00	1/0	64.9	74.9	0.42	22
0.83	5/1	74.1	85.6	0.55	28
0.80	4/1	75.9	87.6	0.58	29
0.75	3/1	78	90.1	0.61	30
0.67	2/1	83.5	96.4	0.68	33
0.50	1/1	95.6	110.4	0.84	40
0.40	2/3	106.5	123.0	0.99	46
0.33	1/3	115.9	133.8	1.11	52

creasing interaxial spacings. Recognizing that the interaxial distance is composed of the diameter of an effective cylinder of water plus a separation  $d_h$ , one can compute the radius  $R_w$  taken on at various DOPE/DOPC ratios as

$$2R_w = s - d_h$$

From data shown in Figure 3b it is estimated that  $d_h$  is approximately 30 Å and is relatively insensitive to the DOPE/DOPC ratio. So in calculating  $R_w$  (Table I), we have assumed  $d_h$  is a constant of 30 Å.

The water to lipid volume ratio is also plotted in Figure 2. Whereas DOPE hexagonal and DOPC lamellar phases take up comparable volumes of water per lipid molecule (Rand et al., 1988), the hexagonal phases with large  $R_w$  can take up two to three times that amount. In the  $H_{II}$  phase, water uptake is driven not only by the hydration of surface groups but also by the demand for a particular spontaneous curvature of the lipid/water interface in the  $H_{II}$  structure. Paradoxically, the larger structures are allowed only because of alkane incorporation, without which the same phospholipid mixture is forced to take on a less hydrated lamellar structure.

The data of Figure 2 are for preparations where 20% of the total added lipid is tetradecane. This may be compared to the interstitial volume between hexagonally packed cylinders. The relation given under Materials and Methods shows that, geometrically, the volume of these interstices is some 9.1% of the total volume of the  $H_{II}$  phase. Using the estimated values of  $d_h$  for the lipid mixtures of Figure 2 and assuming that all the tetradecane occupies the interstices, we compute that as a maximum, for the largest dimension of the 1/2 DOPE/DOPC mixture, 19% of the total lipid needs to be tetradecane. Twenty percent tetradecane then would exceed the amount required to fill the interstices of the hexagonal phases of all these lipid mixtures. The good hexagonal lattice order that allows this computation may reflect the anomalously strong van der Waals force between highly polar cylinders of water.

Table II: Structural Dimensions of DOPE Hexagonal Phases with Varying Amounts of Added Water<sup>a</sup>

$1 - c$	$d_{\text{hex}}$ (Å)	$s$ (Å)	$d_h$ (Å)	$R_w$ (Å)	$R_{pp}$	$d_m$ (Å)	$A_w$ (Å <sup>2</sup> )	$A_{pp}$ (Å <sup>2</sup> )	$A_t$ (Å <sup>2</sup> )
0.06	39.6	45.7	34.1	5.8	17.1	41.1	26	78	104
0.09	42.3	48.8	33.1	7.9	18.6	40.7	32	77	101
0.1	42.9	49.5	33.0	8.3	19.0	40.7	33	77	100
0.12	45.2	52.2	33.0	9.6	20.2	41.1	36	75	97
0.17	48.0	55.4	31.7	11.9	21.9	40.3	41	76	96
0.21	52.9	61.1	31.9	14.6	24.6	41.4	44	74	92
0.23	54.6	63.1	31.4	15.8	25.6	41.2	46	74	92
0.29	60.9	70.3	30.3	20.0	29.4	41.2	51	75	90
0.4	64.2	74.1							
0.5	64.3	74.3							
0.6	64.5	74.5							
0.7	64.7	74.7							

<sup>a</sup> Parameters as described in Figure 1.

Table III: Structural Dimensions of DOPE Hexagonal Phases with 5% Added Tetradecane with Varying Amounts of Added Water

$1 - c$	$d_{\text{hex}}$ (Å)	$s$ (Å)	$R_w$ (Å)
0.16	49.7	57.4	12.0
0.25	59.4	68.6	17.7
0.40	65.3	75.4	
0.50	65.0	75.1	

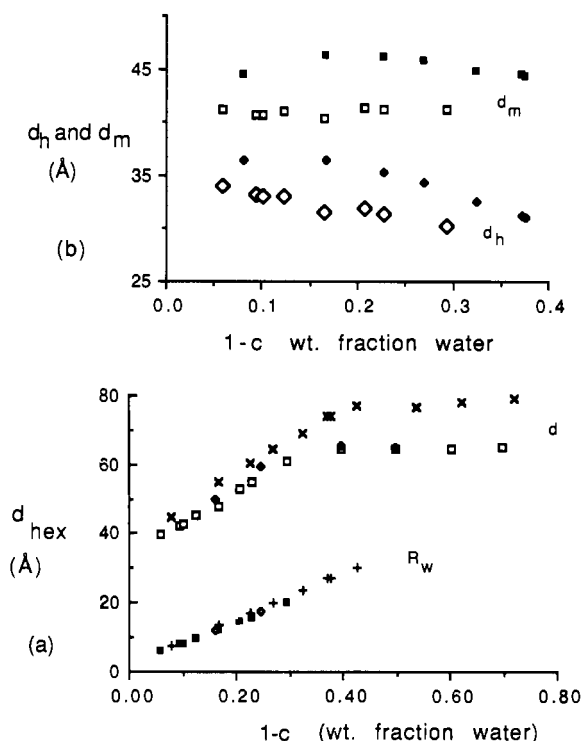


FIGURE 3: (a) Dimensions of the first-order Bragg spacings ( $d$ ) and the water cylinder radii ( $R_w$ ) for the hexagonal phases formed by DOPE with (diamonds) and without (squares) 5% td and of 3/1 DOPE/DOPC with 20% added td ( $\times$  and  $+$ ). These phases form in the indicated weight fraction water. For the mixed lipid system it is estimated (see text) that 12 wt % of the nonaqueous weight is td. (b)  $d_h$  (diamonds) and  $d_m$  (squares) (see Figure 1) are plotted for DOPE (open symbols) and 3/1 DOPE/DOPC with added td (closed symbols) as they vary with water content.

It is not meant to imply that the td statically occupies the interstitial volume.

(b) **Water Stress—No td Stress.** The effects of dehydrating the lipid under conditions where td is in excess are shown by the structural parameters listed in Tables II–IV and illustrated in Figures 3 and 4.

(i) **DOPE.** At 22 °C DOPE forms a single hexagonal phase over the entire concentration range up to at least 94 wt % lipid. The unit-cell dimensions and  $R_w$  increase with increasing water to a constant value at approximately 65 wt % lipid. Thereafter,

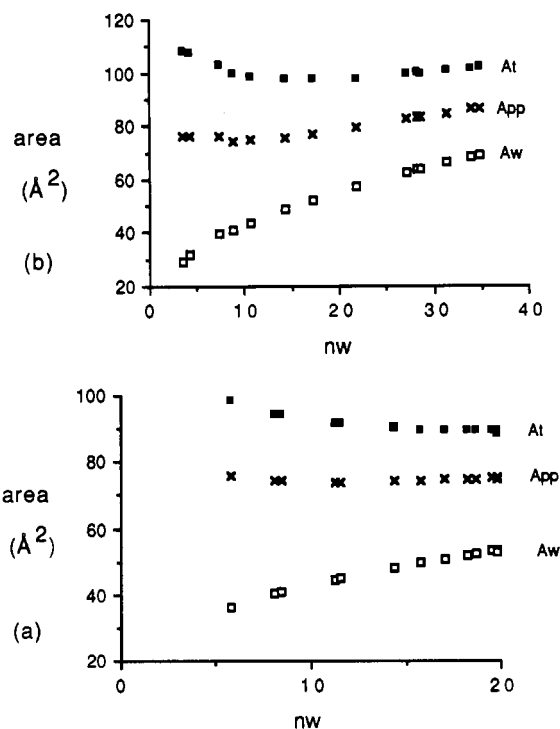


FIGURE 4: Molecular areas calculated at the lipid-water interface ( $A_w$ ), the pivotal position along the length of the phospholipid molecule (see text) ( $A_{pp}$ ), and the end of the monolayer annulus ( $A_t$ ), as they vary with  $n_w$ , the number of waters per lipid molecule. (a) DOPE; (b) 3/1 DOPE/DOPC with added tetradecane assumed to be 12 wt % of the lipid. Note that in both cases the area at the polar group end of the molecule increases while at the ends of the hydrocarbon chains area decreases as water is added and the overall dimension of the hexagonal lattice increases.  $A_{pp}$  on the other hand remains constant.

added water is excess to that taken up by the hexagonal structure. The unit-cell dimensions are those used in determining the dimensions of the osmotically stressed hexagonal phase (Gruner et al., 1986) and agree with those given in Tate and Gruner (1989).

DOPE with 5 (Figure 3a), 10, 15, and 20 wt % td (data not shown), from excess to 10 wt % water, gives pure hexagonal phases with lattice dimensions only very slightly higher than those of pure DOPE. It is not easy to determine if td is in the hexagonal structure. But if pure DOPE in excess water were not at its spontaneous radius of curvature,  $R_0$ , incorporation of td would be expected to show up as a change in the dimension of the hexagonal lattice or in  $R_w$ , as happens so dramatically in the cases of mixtures of DOPC and DOPE. If td were not causing  $R_w$  to change, one would expect the thickness of the hydrocarbon annulus to increase if the td were being taken up by the hydrocarbon chains, assuming that the

Table IV: Structural Dimensions of 3/1 DOPE/DOPC Hexagonal Phases with 20% Added Tetradecane and Varying Amounts of Water<sup>a</sup>

$1 - c'$	$d_{\text{hex}}$ (Å)	$s$ (Å)	$d_h'$ (Å)	$r_w'$ (Å)	$R_{\text{pp}}$	$d_m'$ (Å)	$A_w'$ (Å <sup>2</sup> )	$A_{\text{pp}}'$ (Å <sup>2</sup> )	$A_t'$ (Å <sup>2</sup> )
0.08	44.6	51.5	36.5	7.5	18.3	44.4	33	80	112
0.17	54.7	63.2	36.5	13.4	23.6	46.2	42	75	101
0.23	60.4	69.7	35.3	17.2	27.0	46.1	48	76	98
0.27	64.2	74.1	34.2	20.0	29.3	45.7	52	77	97
0.33	68.8	79.4	32.5	23.5	32.3	44.8	58	80	98
0.37	73.8	85.2	31.2	27.0	35.4	44.4	62	82	98
0.38	74	85.5	31.0	27.2	35.6	44.2	63	82	99
0.43	77	88.9							
0.54	76.6	88.5							
0.62	78.1	90.2							
0.72	78.9	91.1							

<sup>a</sup> The primes show that 12% td is assumed taken up; see text.

Table V: Structural Dimensions of the Lamellar Phase Formed by 3/1 DOPE/DOPC in Varying Amounts of Added Water

$1 - c$	$d_{\text{lam}}$ (Å)	$d_l$ (Å)	$d_w$ (Å)	$A$ (Å <sup>2</sup> )
0.17	48.9	40.6	8.3	60.8
0.20	50.1	40.2	10.0	61.4
0.22	51.3	39.9	11.4	61.8
0.25	52.1	39.2	12.9	62.9
0.28	53.2	38.4	14.8	64.3
0.29	54.3	38.6	15.7	63.8
0.30	53.6	37.6	16.0	65.5
0.33	57.2	38.3	18.9	64.4
0.35	58.1			
0.38	58.0			
0.40	58.2			
0.42	58.1			
0.61	58.3			
0.51	57.6			

volumes of lipid hydrocarbon and td add linearly. This would be reflected in an increase in  $s$ . The fact that  $s$  is nearly constant for 5–20% added td indicates either that only a small part of the td is being taken up by the lipid and the remainder is pooling as bulk td, or that the uptake in td and the concomitant increase in the thickness of the hydrocarbon annulus is being compensated for by a decrease in  $R_w$ .

(ii) *3/1 DOPE/DOPC*. Without td, 3/1 DOPE/DOPC forms a lamellar phase for lipid concentrations up to 83 wt %; its dimensions are shown in Table V. The bilayer thickness over the whole concentration range is between that of  $d_h$  and  $d_m$  of the corresponding hexagonal phases to be described below.

However, upon addition of td, this same 3/1 DOPE/DOPC lipid mixture forms hexagonal phases, and these are seen up to 95 wt % lipid. The amount of td plays a prominent role in driving the lamellar to hexagonal phase transition. At this point we describe only the 20 wt % td case because that level appears to be in excess. By "excess" we mean that additional td has no further effects on the  $H_{II}$  phase behavior or structural dimensions.

Figure 3a shows the dimensions of the single hexagonal phase, over the entire water concentration range, that forms on addition of 20 wt % td to DOPE/DOPC (3/1). There is no appearance of a lamellar phase over the time period of many days at least. The hexagonal phase lattice dimension in excess water is very similar to that with 10 % td (see below). But whether all 20% of the td is accommodated in the final hexagonal phase is difficult to determine. On the basis of more detailed information, shown later in Figure 6, it is estimated that about 12% td is sufficient to saturate this lipid mixture, at least in excess water. On this basis we have concluded that 12% td is the amount incorporated when 20% is supplied, i.e., that td is in excess and the 3/1 lipid mixture is not under td stress for the conditions used in Figure 3. We have calculated the resultant hexagonal phase dimensions assuming 12 wt %

of the lipid is td. The difference between these and the dimensions assuming full 20% incorporation is rather small (equivalent to shifting the data points of Figure 3 to values of  $1 - c$  that are larger by 0.01–0.02) and certainly is insignificant for the use of these data in the application to the water stress data to follow.

Figure 3b shows the range in lengths the molecules must occupy in the hexagonal phase assuming the water cylinders are circular in cross section. This range of lengths in the single DOPE/DOPC 20% td phase is compared with that of pure DOPE. Over the whole range of water concentrations  $d_m$  is remarkably constant in both lipid systems. Both  $d_h$  and  $d_m$  are larger in the mixed-lipid system compared to DOPE. The increase in  $d_m$  is expected, since td relaxes the stress associated with the interstices, but there is also an increase of 2–3 Å in  $d_h$ , the intercylinder distance. To what extent these increases are attributable to the increased average size of the polar groups and how much to the added td is not known. If one computes the lipid or nonaqueous volume fraction in the shaded region of Figure 1 over the range of water concentrations of Figure 3b, one finds that it amounts to 10–15% of the total lipid.

Figure 4 shows the average molecular areas at three positions, from the polar group–water interface out to the periphery of the lipid annulus. It is surprising to note that the changes in molecular area go in opposite directions at each end of the molecule as the hexagonal lattice is decreased under water stress. At the polar group–water interface the area decreases as water is withdrawn, consistent with all observations on liquid crystalline phases. However, at the ends of the hydrocarbon chains the areas increase with dehydration. So the molecules are compressed at their polar ends but splay at the hydrocarbon chain end as the monolayer is bent to smaller radii of curvature. Combined with the concomitant changes in  $d_h$  and the constancy of  $d_m$  on dehydration, these results suggest that if the cylinders are circular in cross section, then molecules aligned in the direction of the interstices and those in the direction between the cylinder centers undergo different shape changes. Evidence for circular symmetry within 2-Å resolution has been seen for DOPE (Turner & Gruner, 1989).

Importantly, at some intermediate distance along the length of the molecule there appears to be a neutral or pivotal position where there is little change in molecular area with dehydration. For the 3/1 mixture the pivotal position was taken where the variation in area with dehydration was a minimum. Such a pivot suggests that the monolayer radius of curvature should be defined at this position. As described under Discussion this pivotal position gives a spontaneous radius of curvature at  $R_0 = 31.5$  Å for DOPE in excess water and at  $R_0 = 37.8$  Å for the 3/1 DOPE/DOPC mixture again in excess water and td. These radii then define a volume fraction of each phospholipid molecule to be included inside a cylinder whose radius is de-

Table VI: Dimensions of the Phases Formed by 3/1 DOPE/DOPC with Varying Amounts of Tetradecane and Excess Water

wt % td in DOPE/DOPC	$d_{\text{hex}}$ (Å)	$d_{\text{lam}}$ (Å)
3.6	73	59
4.4	72.7	59
5	74.6	59.7
8.4	76.1	60
10.9	77.8	60.9
11	78.6	
11.8	78.5	
12.7	78.7	
15	79.1	
18	77	
20.8	78.1	

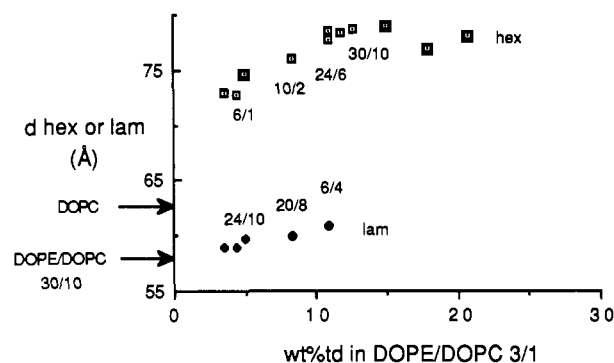


FIGURE 5: Lamellar and hexagonal phase dimensions (first-order Bragg spacings) for 3/1 DOPE/DOPC mixtures in excess water with varying amounts of added td. The two phases coexist over the range of 3.6–10.9% added td (see Table VI). On the basis of a global DOPE/DOPC ratio of 30/10 in all samples, and using data from Figure 2, we have estimated the DOPE/DOPC ratios of each phase in the mixed-phase region. The relative amounts of each phase, indicated by the sum of the values in each ratio of the lamellar and hexagonal phases, are consistent with the relative amounts of each phase estimated from the X-ray diffraction intensities. The dimensions of each phase are also consistent with previous measurements of DOPE/DOPC mixtures. Note that the DOPE/DOPC ratios decrease, i.e., DOPC content increases, in both phases as the td content increases. We argue in the text that the lipid demixes and adjusts the composition of the hexagonal phase to minimize chain stress by matching its  $R_0$  to the available td.

creased when water is removed and the monolayer bent from  $R_0$ .

(c) *Excess Water-td Stress.* Phase separation in excess water, driven by td stress, is shown by the data in Table VI and Figure 5 and discussed formally in the appendix.

At a 3/1 ratio, DOPE/DOPC with no td forms a lamellar phase in excess water (Table V). Tetradecane added to excess converts this lamellar phase into a hexagonal  $H_{II}$  structure, as described above. At limiting levels of tetradecane, the lipid segregates into lamellar and  $H_{II}$  phases whose lattice dimensions and compositions differ from those at zero or excess td.

In the two-phase region of Figure 5, as the amount of added td is increased from 3 to 11 wt % of the lipid, an increasing proportion of the lipid forms the hexagonal structure. Coexisting with this hexagonal phase is a lamellar phase of repeat spacing always greater than the 58-Å lamellar spacing formed by DOPE/DOPC, 3/1, without td. Increasing td results in a small but progressive increase of the dimensions of the coexisting lamellar phase in a direction that approaches the repeat spacing of pure DOPC.

Tetradecane has a greater effect on the dimensions of the  $H_{II}$  phase. Even at 3% td, the Bragg spacing of nearly 73 Å is much greater than the 64.5-Å spacing for pure DOPE. By 11% td, this distance has grown to 78 Å. Further addition of td causes no change in hexagonal lattice spacing; there is also no sign of a lamellar structure.

Table VII: Dimensions of the Lamellar and Hexagonal Phases Formed by 3/1 DOPE/DOPC with 5% and 10% Added Tetradecane and Varying Amounts of Water

with 10% tetradecane			with 5% tetradecane		
1 - c	$d_{\text{hex}}$ (Å)	$d_{\text{lam}}$ (Å)	1 - c	$d_{\text{hex}}$ (Å)	$d_{\text{lam}}$ (Å)
0.15	49.3		0.15	48.5	
0.20	56.2	52.2	0.11	44.6	
0.25	62	53.3	0.24	62.8	53.2
0.31	70.7	55.6	0.29	68.8	55.1
0.35	73.2	57	0.34	70.7	56.7
0.40	75.6	58.5	0.45	75.1	60.8
0.45	77	60.6	0.50	74.9	60.2
0.50	79.5		0.60	74.1	60.2
			0.70	74.6	59.7

We take these data as evidence to suggest the following: (a) At less than 11–12 wt % td, the hexagonal phase is under stress from limited alkane. (b) td in excess of 12 wt % does not associate with the phospholipid mixture in a structurally or energetically important way. (c) PE/PC ratios adjust with limited td in such a way as to minimize curvature energy and maximize entropy of phospholipid mixing; the stress of limited alkane is felt as a force for demixing lipids. This last point is essential to the role we believe the balance between the water and alkane stresses plays in organizing lipid structures.

Where solvent stress results in segregation into two phospholipid phases, the composition of each phase is unknown. However, the sensitivity of the relation between unit-cell dimensions,  $R_w$ , and composition as seen in Figure 2 allows an estimate of the DOPE and DOPC ratios in the separate phases. We have applied this approach to estimate the phase composition in the following way. We assume in that estimation that, at equilibrium, the lipid has segregated so that the coexisting hexagonal phase contains all the td and has adjusted its composition to be stress-free and achieved a spontaneous radius  $R_0$ , as if now both solvents are in excess for the hexagonally packed fraction. [Of course one expects the td to partition between coexisting  $L_a$  and  $H_{II}$  phases. The fact that td has very little effect on the lamellar repeat spacing (e.g., Table VII) suggests that td does not readily partition into the lamellar phase. However, it is cautioned that the relative partitioning of td into bulk td,  $L_a$ , and  $H_{II}$  phases has not been directly measured in this study.] By reference to the data of Figure 2 the hexagonal spacing can give the DOPE/DOPC ratio for such a hexagonal phase. That estimated ratio is indicated on Figure 5 and decreases as the td content increases. This is consistent with  $R_0$  increasing with increasing DOPC content. This strongly suggests that the hexagonal phases of the segregated lipids, at the intermediate and increasing td levels, are those of *increasing* DOPC content.

In a similar manner we estimate the composition of the coexisting lamellar phases of Figure 5 from their dimensions. Mixtures of DOPE/DOPC in decreasing ratios from 3/1, without added tetradecane, form lamellar phases whose dimensions systematically increase, very nonlinearly, and approach that of pure DOPC (Rand et al., 1988). By reference to the lamellar repeat spacings of DOPE/DOPC 3/1, and of DOPC (arrows in Figure 5), the systematic increase in the dimensions of the coexisting lamellar phase, with increasing td content, is of the magnitude expected for the ratios shown in Figure 5. These ratios indicate, surprisingly, that these coexisting lamellar phases, like the hexagonal phases, also have *increasing* DOPC content as shown in Figure 5. How can both coexisting lamellar and hexagonal phases increase their DOPC content as td content increases, when the global DOPE/DOPC ratio in all samples is fixed at 3/1? It is possible if the lamellar/hexagonal mass ratio changes. This is what is observed



Table VIII: Relation between the Osmotic Stress and the Structural Parameters of the DOPE Hexagonal Phase

$\log P$ (dyn/cm <sup>2</sup> )	$d_{\text{hex}}$ (Å)	$1 - c$	$s$ (Å)	$R_w$ (Å)	$R_{\text{pp}}$ (Å)	$V_w$ (Å <sup>3</sup> )	$A_w$	$A_{\text{pp}}$	$A_t$
8.49	39.9	0.07	46.1	6.4	17.4	93	29	78	104
8.35	40.6	0.08	46.9	6.8	17.7	101	30	78	103
7.92	44.7	0.12	51.6	9.5	20.0	173	36	76	98
7.68	48.9	0.17	56.5	12.0	22.3	244	40	75	95
7.59	49.3	0.17	56.9	12.3	22.5	253	41	75	94
7.29	53.7	0.22	62.0	15.1	25.0	338	45	74	92
7.22	54.1	0.22	62.5	15.4	25.3	348	45	74	91
7.04	57.8	0.26	66.7	17.9	27.5	433	48	74	90
6.88	59.5	0.28	68.7	19.0	28.5	473	50	74	90
6.65	60.9	0.29	70.3	20.0	29.4	514	51	75	90
6.48	62.4	0.31	72.1	21.0	30.2	549	52	75	89
6.16	62.9	0.31	72.6	21.3	30.6	562	52	75	89
6	63.7	0.32	73.6	20.9	31.1	586	53	75	89
5.8	64	0.33	73.9	22.1	31.2	594	53	75	89
5.41	64.6	0.33	74.6	22.3	31.5	594	53	74	89

Table IX: Relation between the Osmotic Stress and the Structural Parameters of the Hexagonal Phases Formed by 3/1 DOPE/DOPC Containing 12% Tetradecane (Assumed Taken Up from 20% Added Tetradecane: See Text)

$\log P$ (dyn/cm <sup>2</sup> )	$d_{\text{hex}}$ (Å)	$1 - c$	$s$ (Å)	$R_w$ (Å)	$R_{\text{pp}}$ (Å)	$V_w$ (Å <sup>3</sup> )	$V_w/\text{pe}$ (Å <sup>3</sup> )	$A_w$	$A_{\text{pp}}$	$A_t$
8.49	45.5	0.07	52.5	7.1	18.5	105	101	29	77	108
8.35	46.6	0.08	53.8	8.0	19.1	127	121	32	76	107
7.76	51.4	0.14	59.4	11.3	21.8	223	214	39	76	103
7.69	51.4	0.14	59.4	11.3	21.8	223	214	39	76	103
7.54	54.6	0.16	63.1	12.9	23.5	265	254	41	74	100
7.4	56.8	0.18	65.6	14.6	24.8	320	307	44	75	99
7.21	61	0.23	70.4	17.6	27.3	428	410	49	76	98
7.02	63.7	0.27	73.6	19.7	29.0	516	494	52	77	98
6.76	68.0	0.32	78.5	22.9	31.8	654	626	57	79	98
6.43	71.7	0.36	82.8	25.9	34.3	813	778	63	83	100
6.15	73.1	0.38	84.4	26.9	35.2	861	824	64	83	100
5.99	72.6	0.37	83.8	26.6	34.9	850	813	64	83	100
5.48	77.1	0.42	89.0	30.1	37.9	1043	998	69	87	102
6.00	74.6	0.40	86.1	28.2	36.2	938	898	66	85	101
5.94	73.1	0.38	84.4	26.9	35.2	861	824	64	83	100
5.7	76.6	0.42	88.5	29.7	37.5	1021	977	69	86	102
5.28	76.6	0.42	88.5	29.7	37.5	1021	977	69	86	102
4.84	77	0.42	88.9	30.1	37.8	1043	998	69	87	102

and described by the estimated ratios in Figure 5. For all samples with a DOPE/DOPC global mole ratio of 30/10, the DOPE/DOPC ratios in both phases decrease while the amount of lipid in each phase, proportional to the sum of the numerator and denominator in each ratio, changes in opposite directions.

(d) *Water Stress and td Stress.* Phase separation under conditions of both water and td stress is shown by the data in Table VII. DOPE/DOPC, 3/1, mixed with 5 wt % td produces coexisting lamellar and hexagonal phases, with increasing proportion of lamellar phase on the time scale of several hours. The relatively rapid kinetics of formation of the coexisting phases indicate a strong drive toward lipid segregation. The dimension of the 3/1 hexagonal phase in excess water is much larger than that of pure DOPE. Preparations with 10 wt % td initially show a single hexagonal phase of larger dimensions, in excess water, than that seen for 5% td. But after some 2–3 days a coexisting lamellar phase appears consistently, a clear indication of slow lipid segregation. Recall that at 20% td there is no td stress, and a single hexagonal phase is observed. We take the kinetics of separation as a measure of the stress within the single hexagonal phase that first forms and which drives lipid segregation as the lipid composition adjusts to the available td. On this basis that stress should increase the lower the amount of td and the further from the spontaneous radius  $R_0$  the lipid is constrained to be.

(While we cannot absolutely eliminate the possibility that the longer time scale phase separation results from a small amount of lipid decomposition, several observations strongly suggest that this is not so. Thin-layer chromatography of

samples much older than 3–4 days show no decomposition. Both the rate of phase separation and the dimensions of those phases are proportional to the amount of added td and not to the age of the sample. Furthermore, samples weeks old in excess td show no phase separation or detectable decomposition.)

The shift from a two-phase to a one-phase system seen on adding td beyond 10% again shows that this 3/1 lipid mixture spontaneously accommodates more than 10% td. At low water contents for all levels of td however, there is a single hexagonal phase. The small change in the dimensions of this single phase with td content, seen at  $1 - c = 0.15$ , indicates an increased affinity for td beyond 10%. These single hexagonal phases at low water content are a long way from their spontaneous  $R_0$  and are under both water and, with the exception of the “20%” td case, td stress. Again, we interpret the cases where the lipid segregates into two phases as evidence of a strong tendency to minimize bending energy by adjusting lipid composition, and consequently  $R_0$ , to the available td.

*Osmotic Stress of These Lipid Systems.* In those cases where there is only one hexagonal or lamellar phase, the exerted osmotic stress was measured vs the volume of water,  $V_w$ , per lipid molecule, normalized to the mass of the DOPE polar group, Figure 6. For pure DOPE, which spontaneously forms an  $H_{II}$  phase at room temperature (Table VIII), and for the 3/1 DOPE/DOPC mixture induced to become hexagonal by the addition of 20 wt % tetradecane (Table IX), there is a remarkable equality of osmotic stress vs water volume for  $V_w < 400$  Å<sup>3</sup>. It seems that there is virtually no effect of the methylated polar groups of DOPC when the pore is closed

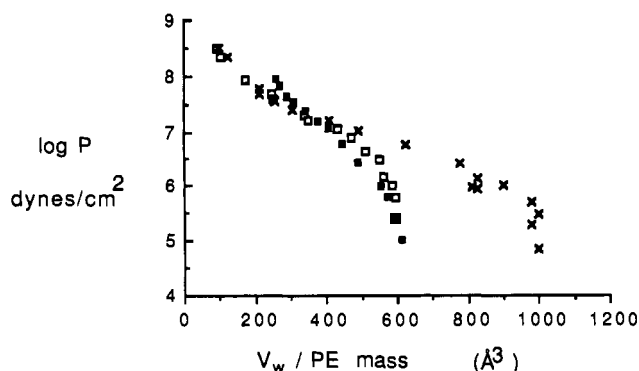


FIGURE 6: Variation in the volume of water per DOPE polar mass with osmotic stress for DOPE alone (open squares), for 3/1 DOPE/DOPC lamellar phase (closed squares), and for the hexagonal phase formed by 3/1 DOPE/DOPC with 20% added td (crosses).

Table X: Relation between the Osmotic Stress, or Interbilayer Pressure, and the Structural Parameters of the Lamellar Phase Formed by 3/1 DOPE/DOPC

log <i>P</i> (dyn/cm <sup>2</sup> )	<i>d<sub>w</sub></i> (Å)	<i>d</i> (Å)	<i>V<sub>w</sub></i> (Å <sup>3</sup> )	<i>A<sub>w</sub></i>
7.92	9.0	49.5	273	60.0
7.79	9.3	49.6	283	61.1
7.62	9.8	50.0	302	61.4
7.53	10.4	50.5	321	61.6
7.37	11.5	51.1	357	62.2
7.19	12.5	51.8	393	62.8
7.04	13.5	52.4	426	63.3
6.76	15.5	53.1	465	64.0
6.43	15.9	54.1	514	64.5
5.97	17.9	55.9	581	64.8
5.78	18.5	56.5	600	64.9
5.41	19.3	57.2	627	64.9
5.02	19.7	57.6	641	65.0

down to these water contents. At lower pressures and larger radii however, there is a clear divergence of the force curve for the PE/PC mixture from that of pure DOPE, concomitant with the much larger uptake of water by the mixture.

Compared with similar measurements on the lamellar phase of the 3/1 mixture without alkane, Figure 6 and Table X, these data show that the 3/1 lamellar phase takes up far less water than does its hexagonal counterpart. In addition, at higher pressures, it takes more work to dehydrate the lipid in the lamellar phase. The geometry of packing therefore seems to have an important effect in lipid hydration over the whole range of water contents.

## DISCUSSION

The results presented here demonstrate that the solvent affinity of  $H_{II}$  phases has some mechanism in addition to the local solvation processes which are normally thought of as responsible for the solvent affinity of solutes, or of open, isolated hydrophilic surfaces. In the latter cases "solvent affinity" means the solvent-solute or solvent-surface interactions driven by local mechanisms which lower the system free energy in the presence of the solvent. Affinity for water typically arises because charged groups can lower the free energy by immersion in a medium of high polarizability, or because groups can hydrogen bond to water. Certainly in both lamellar and hexagonal phases much of the affinity for waters within a few angstroms of the phospholipid headgroups arises from such local mechanisms.

However, a second mechanism of solvent affinity must be used to explain the large additional amounts of water taken up by the  $H_{II}$  phase, especially when the water core is large. The mechanism effecting such solvent uptake is nonlocal in that it results more from the geometry of the lipid layers than

directly from the chemical properties of the lipid surfaces. This additional nonlocal solvation mechanism arises when the spontaneous curvature of the lipid monolayers would be at a free-energy minimum in a geometry which would create voids or low-density regions in the liquid crystalline structure, voids that are filled with compatible solvent. Without enough water, the hydrophilic cores of the  $H_{II}$  phase shrink; without enough alkane, the  $H_{II}$  phase will often simply cease to exist.

To illustrate this mechanism, consider the gradual removal, by osmotic stress, of water from an  $H_{II}$  phase in which the water core is many water molecules across. One energetic cost of removing water might be due to bending of the lipid monolayers, given to a first approximation by the quadratic function

$$(1/2)K_0(1/R - 1/R_0)^2$$

per unit area of interface (Kirk et al., 1984). This is the expected form for the energy of bending a surface from a minimum energy radius,  $R_0$ , to a radius  $R$  against a bending (rigidity) modulus  $K_0$  [i.e., Helfrich (1973)]. This curvature energy involves only the energy of bending the lipid monolayer to a smaller radius with the removal of void-filling water from the center of the water cores. It omits any energetic cost of locally dehydrating the polar groups. We have argued earlier (Gruner et al., 1986), and will pursue this point here, that this is a reasonable assumption when the center of the fully hydrated water core is far enough from the mean headgroup surface.

The "solvation" of the phospholipid  $H_{II}$  phases by both water and oil solvents, as examined in this paper, illustrates the way the amphiphile physically mediates its interaction with two kinds of solvent. The interaction is particularly noticeable for DOPE/DOPC mixtures of relatively high DOPC content in excess water and tetradecane. Increasing the fraction of DOPC concomitantly increases the water content and the spontaneous radius of curvature of the lipid monolayers (Figure 2). The presence of tetradecane, which compatibly occupies volume among the lipid chains, allows formation of the spontaneous curvature as an  $H_{II}$  phase. This formation in turn requires more water to fill the large radius of water pores. Quite logically, then, the addition of alkane increases affinity for water.

In contrast, the volume requirements of the lamellar phase for water are much more closely coupled to the local hydration of the lipid headgroup surfaces. In fact, one expects that the local affinity for water, in the sense of directly hydrating the headgroups, is much the same in both lamellar and  $H_{II}$  phases. What distinguishes the two phases, with respect to water affinity, is the different geometries of the water cavities.

With respect to the distribution of alkane in an  $H_{II}$  phase, one should not imagine that these solvents fill cleanly structured voids and remain in well-defined, restricted positions. Indeed, entropy will tend to drive oil molecules to diffuse over a large volume of the phospholipid acyl chain region. The "oil voids" are better understood as a net measure of the extra volume required in the chain region if the lipid layers are to bend to energetically favorable radii of curvature. It has certainly not yet been established that the oil molecules spend a large fraction of time in the relatively small interstitial volumes of the hydrocarbon zone. It does seem clear, though, that a volume of oil equal to the volume of an ideal missing interstitial volume allows hydrophobic material, oil or acyl chain, to fill the required region. One should further not assume that all alkanes are equivalent. The curvature model to which the data of this paper are being applied is a phenomenological model which treats the hydrocarbon region as a



continuous medium and which ignores fine tuning due to specific molecular interactions that might be expected. For example, Sjolund et al. (1989) have recently shown that although different length normal alkanes can induce the  $H_{II}$  phase in various PC's, the fraction of the PC in a hexagonal phase for a given weight fraction of alkane varies systematically with alkane length. It would, in fact, be of great interest to determine the relative partitioning of oil and lipid chains into the interstitial volumes.

**Bending Energy of the  $H_{II}$  Monolayer.** The plots of molecular cross-sectional area given in Figure 4 suggest clearly that there exists a position along the phospholipid molecule at which there is little change in molecular cross-sectional area with dehydration and deformation of the hexagonal phase. Such a position must represent a pivot where, on bending the monolayer, the polar end of the molecule is compressed and the hydrocarbon end is expanded. We determine that position as the location which, when a constant volume of the phospholipid molecule is included with the water volume, gives the constant or near-constant areas in Figure 4. For both DOPE and 3/1 DOPE/DOPC that volume included the polar group and 0.3 of the volume of the hydrocarbon chains. In our earlier study (Gruner et al., 1986) we defined the radius of curvature of the monolayer as the maximum radius of the water cylinder that encompassed all the water but none of the lipid. In contrast, we now define the radius of curvature as the distance,  $R_{pp}$ , from the water cylinder axis to the nearly constant-area pivotal position along the phospholipid molecule. By this definition we compute spontaneous radii of curvature, in excess water and tetradecane, of 31.5 and 37.8 Å for pure DOPE and 3/1 DOPE/DOPC mixtures, respectively. Because of the constancy of area at this pivotal position, we can now use this new definition of radius of curvature to test the accuracy of a quadratic form of the bending energy per unit area in describing the work of water removal from the hexagonal lattice. Specifically, as before (Gruner et al., 1986), we test the form

$$g(r) = (K_0/2)(1/R_{pp} - 1/R_0)^2$$

for the energy per lipid molecule. The osmotic stress  $P$  is the rate of change of energy  $g$  with respect to the volume of water  $V_w$  per lipid molecule:

$$P = dg/dV_w = (dg/dR_{pp})(dR_{pp}/dV_w)$$

The total volume,  $V_{pp}$ , falling within the cylinder surface defined at the pivotal point is the cross-sectional area  $A_{pp}$  divided by the surface to volume ratio  $2/R_{pp}$ . This includes  $V_w$  plus a constant volume  $V_{ph}$  of the included part of the phospholipid molecule. Because  $V_{ph}$  is constant, the derivative  $dV_w/dR$  is equal to the derivative of total volume  $V_{pp} = V_{ph} + V_w$ . Specifically

$$V_{pp} = A_{pp}R_{pp}/2$$

$$dV_w/dR_{pp} = dV_{pp}/dR_{pp} = A_{pp}/2$$

The contribution of bending energy to the osmotic pressure of the lattice is then

$$P = K_0(1/R_{pp} - 1/R_0)(-1/R_{pp}^2)/(A_{pp}/2)$$

Rearranging terms yields a linear relation between  $R_{pp}^2P$  vs  $1/R_{pp}$ :

$$\begin{aligned} R_{pp}^2P &= (2K_0/A_{pp})(1/R_0 - 1/R_{pp}) \\ &= K_c(1/R_0 - 1/R_{pp}) \end{aligned}$$

We have introduced the modulus  $K_c = 2K_0/A$  first to convert an energy per molecule to an energy per area and

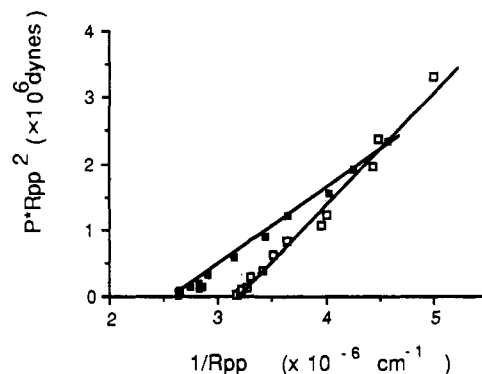


FIGURE 7: Test of the quadratic bending energy formula  $R_{pp}^2P = K_c(1/R_0 - 1/R_{pp})$  using the osmotic stress data of Tables VIII and IX. The highest two osmotic pressure points deviate from the trend and were excluded from the fit. Best-fit linear plots yield  $K_c = 1.7 \times 10^{-12}$  ergs (41.7 kT) and  $R_0 = 30.9$  Å for DOPE (open squares) and  $K_c = 1.2 \times 10^{-12}$  ergs (29.5 kT) and  $R_0 = 37.5$  Å for DOPE/DOPC with 12% td (closed squares).

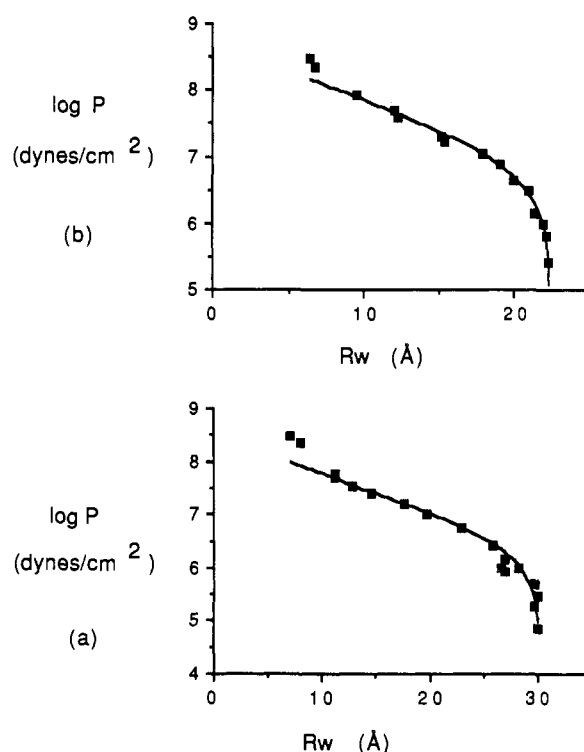


FIGURE 8: Variation in the radius of the water cylinder with osmotic stress for the hexagonal phases of DOPE (a) and for 3/1 DOPE/DOPC (b). Comparison of experimentally measured values (filled squares) with those expected (continuous line) by fitting the quadratic form of the monolayer bending energy with the parameters derived in Figure 7.

second, through the factor of 2, to be a modulus appropriate for bending two monolayers. This last conversion allows comparison with bending of bilayers under the assumption that the two halves of the bilayer are uncoupled during bending.

We test the quadratic bending energy formula by plotting osmotic stress data as  $R_{pp}^2P$  vs  $1/R_{pp}$ , in Figure 7, from the data of Tables VIII and IX. These data so plotted give a remarkably straight line for all but the highest osmotic pressures. From the slopes and intercepts, we obtain  $K_c = 1.7 \times 10^{-12}$  ergs (41.7 kT) and  $R_0 = 30.9$  Å for pure DOPE and  $K_c = 1.2 \times 10^{-12}$  ergs (29.5 kT) and  $R_0 = 37.5$  Å for 3/1 DOPE/DOPC. (There is a slight disparity between the  $R_0$ 's so obtained and the  $R_0$ 's directly determined by structural analysis which are 31.5 and 37.8 Å.) This agrees well with

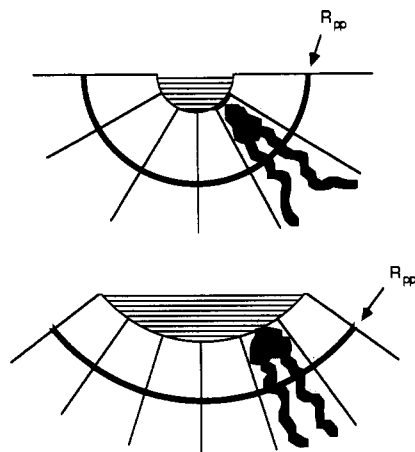


FIGURE 9: Scale drawing of monolayers in the minimally and the maximally hydrated DOPE hexagonal phase. The outlined radial sectors, surrounding the central water cores, represent cross sections of constant-thickness slabs, in the direction of the cylinder axis, which delimit the excluded volumes of single DOPE molecules. The changes in sector dimensions illustrate that when the monolayer is bent, the areas of the polar and hydrocarbon ends of the molecule change in opposite directions as the molecule pivots around a position of constant area,  $R_{pp}$ . That position, the neutral plane of the monolayer, is indicated by the thicker circumferential line and is one-third of the distance along the hydrocarbon chain from the polar group. (Changes in molecular area can result from changes in dimension parallel to the cylinder axis, along the cylinder circumference, or both. Whichever way area changes are attributed does not change the neutral plane. In this drawing, the slab thickness has been taken as constant during monolayer bending.)

$K_c$  values obtained for bilayers by other means [e.g., see Bo and Waugh (1989)].

As shown in Figure 8, a quadratic bending energy with these derived parameters fits the measured force curves over a large range of dehydration of the hexagonal phase. These moduli are larger than those we estimated earlier (Gruner et al., 1986), using as a definition of the radius of curvature the polar group–water interface, and now are very close to recent estimates in lamellar systems (Duwe et al., 1987) and for phospholipid vesicles (Schneider et al., 1984).

Figure 9 is a scale drawing of the cross section of DOPE monolayers, in the minimally and maximally hydrated DOPE hexagonal phase. It illustrates the change in opposite directions that the areas of the polar and hydrocarbon ends of the molecule undergo when the monolayer is bent and the molecules pivot around their position of constant area,  $R_{pp}$ .

We point out that even though the measured energies fit so well with a quadratic energy of curvature, this does not exclude the possibility that other kinds of interaction or functional forms might give an equally good description of the data.

**Interactions at Low Hydration.** Deviation from the quadratic form at very low water contents is positive (Figure 8). It is more difficult to remove water in this limit than what is predicted by bending alone. At such low water contents, three to five waters per phospholipid, one expects local hydration affinity to contribute significantly to dehydration energies.

It appears also, in Figure 6, that in this high osmotic stress, low water content region where bending energy no longer suffices to explain the work of water removal from the hexagonal phase, that it is somewhat more difficult to remove water from the same polar groups when they are arranged in the lamellar phase. We had argued previously, on the basis of what we judged to be comparable forces for different lamellar and hexagonal phases, that in that crowded world of polar groups one could speak of a "polar mash" whose prop-

erties did not depend strongly on the shape of the surface to which they were anchored. Now having measured a difference in the  $P$  vs  $V_w$  for 3/1 DOPE/DOPC mixtures in the  $H_{II}$  and lamellar geometries, this equivalence appears not to be so. In addition, if one converts the volume per lipid into molar units for polar group concentration, one sees immediately that these groups are at concentrations far exceeding their saturating values for free polar groups in solution (Schumaker & Sandermann, 1976). This inequality was noted for lamellar phases (Rand et al., 1988) and seems to be true as well for hexagonal phases. One is presented with the paradox that polar groups hydrate more strongly by virtue of being attached to nonpolar acyl chains. They also seem to hold onto water more strongly when attached to a planar surface than to one with a concave curvature. We take this as yet another example of the importance of geometric constraints, at least those of concave surfaces, on solvent affinity.

**Phase Separation of DOPE/DOPC Mixtures.** In excess water and under conditions where there is a limited amount of added alkane, DOPE/DOPC lipid mixtures can separate spontaneously into lamellar and hexagonal phases. One may think of the phase separation data as due to the incorporation of tetradecane into a hexagonal phase whose composition, dimensions, and amount optimally use all available alkane. This hexagonal phase is expected to be near its spontaneous radius of curvature and under little bending strain. The monolayers in the lipid that remains in lamellar phase, due to a lack of filler alkane, suffer a strain of bending away from the spontaneous curvature that they would prefer. Given the constraint that almost all tetradecane is in the hexagonal structure, the system optimizes its free energy by changing the PE/PC ratio in each of the phases. There is a balance between bending energy in the lamellar phase and an entropy of demixing the lipids into the individual phases. This balance between bending energies and mixing entropies provides a qualitatively correct rationale for the observed phase separation as shown in the Appendix. However, it is still too early to test such a relation quantitatively. Such a test requires that one has established at each global PE/PC ratio, precisely known relative amounts and lipid ratios of each of the separated phases, well-defined  $R_0$ 's for the hexagonal phases, and knowledge of the fraction of td in each phase.

The inherent amphiphilic nature of membrane phospholipids creates affinities for both hydrophobic and hydrophilic solvents. Recognition of dual-solvent affinities is important for understanding properties of natural membranes whose composition involves a variety of lipid types and which are exposed to a variety of polar and nonpolar materials. The capacity of the ends of very long chain lipid molecules to fill the space required by nonlamellar structures suggests they can play the same major but little-recognized role in lipid polymorphism as do the hydrocarbon molecules in this study. They may then be energetically important in hydrocarbon packing around intrinsic proteins and in membrane-disrupting events such as endocytosis and fusion.

#### ACKNOWLEDGMENTS

We thank D. Turner for useful discussions on the structure of the lipid mesomorphs.

#### APPENDIX

The following is a model to illustrate how a mixture of PE, PC, and oil (td) can partition between coexisting lamellar and hexagonal phases in such a manner that the PC concentration of both phases increases with oil concentration. The model is based on the competition between the curvature energy of

the lipid layers and the entropy of mixing with the degree of freedom such that the two phases can adjust the spontaneous curvatures by seeking different PE to PC ratios. The model is based on the following assumptions: (a) The curvature energy in the lamellar phase is  $K_c/2R_0^2$ , and the lamellar phase has zero hydrocarbon packing energy. (b) All the lipid is constrained to be in the  $H_{II}$  phase in such a manner as to eliminate energy contributions due to hydrocarbon packing. (c) The  $H_{II}$  phase has a zero curvature energy contribution when  $R = R_0$ . (d) Entropy contributions due to partitioning of the oil and water are ignored.

Clearly these assumptions are simplifications of constraints imposed on the real system, and therefore, the model should be viewed as simply qualitative and illustrative. However, we believe that a more rigorous model, once functional forms for energies such as hydrocarbon packing energy and curvature energy for flat lamellae are known, would follow essentially the same steps.

We formulate a free energy based on (1) the energy of bending and (2) the entropy of molecular mixing.

(1) There is positive energy stored in the lamellar form by virtue of lipids being forced out of the hexagonal structure they would have formed in excess alkane and water. This bending energy is taken as a quadratic function (Gruner et al., 1986):

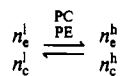
$$(1/2)K_c/R_0^2 \text{ per unit area}$$

$K_c$  is the bending modulus and  $R_0$  the spontaneous radius of curvature in excess solvents. We assume that there is relatively negligible bending energy in the lipids in that part of the system in inverted hexagonal form which have taken up alkane.

There is an entropy of demixing of PE and PC from the original ratio to the individual ratios they assume in the lamellar or hexagonal phase. This entropy is computed by standard "number of ways" methods. The free energy is minimized under the constraint that all available alkane goes into the  $H_{II}$  structure, a constraint that is suggested by the negligible effect of added alkane on the lamellar structure.

We take the following notations:  $n$  = the total number of phospholipid molecules,  $l$  and  $h$  superscripts designating lamellar and hexagonal forms and  $e$  and  $c$  subscripts designating PE and PC;  $\rho$  = PE/PC ratio in original mixture;  $\rho^l$  and  $\rho^h$  = PE/PC ratios respectively in lamellar or hexagonal phase;  $S$  = surface area per molecule.

We compute the ratios  $\rho^l$  and  $\rho^h$  by considering the free energy change that occurs upon swapping a PC and a PE molecule between lamellar and hexagonal phase. When this change is zero, the system has achieved the most favorable composition for each phase:



In this swap, the total number of molecules,  $n^l = n_e^l + n_c^l$  and  $n^h = n_e^h + n_c^h$ , is kept fixed.

**Change in Bending Work.** From measurements we know what  $R_0$  would be for a particular PE/PC ratio in excess alkane; i.e., we know

$$R_0(\rho^l)$$

The bending energy for the lamellar fraction is

$$n^l S^l \frac{K_c}{2} \frac{1}{R_0^2(\rho^l)}$$

We compute the change in  $\rho^l$  and  $R_0$  with a swap to change  $\rho^l = n_e^l/n_c^l$  to

$$\rho^h = \frac{n_e^h - 1}{n_c^h + 1} = \frac{n_e^l \left(1 - \frac{1}{n_c^l}\right)}{n_c^l \left(1 + \frac{1}{n_c^l}\right)} \approx \rho^l \left(1 - \frac{1}{n_c^l} - \frac{1}{n_c^l} + \dots\right) = \rho^l - \frac{1 + \rho^l}{n_c^l}$$

$$\frac{\partial R_0}{\partial \text{swap}} = \frac{\partial R_0}{\partial \rho^l} \frac{\partial \rho^l}{\partial \text{swap}} = \frac{\partial R_0}{\partial \rho^l} \left(-\frac{1 + \rho^l}{n_c^l}\right)$$

where  $\partial R_0/\partial \rho^l$  is a known (-) quantity.

$$R_0(\rho^h) = R_0(\rho^l) + \frac{\partial R_0}{\partial \rho^l} \left(-\frac{1 + \rho^l}{n_c^l}\right)$$

$$R_0^2(\rho^h) = R_0^2(\rho^l) \left[1 - \frac{2 \frac{\partial R_0}{\partial \rho^l} (1 + \rho^l)}{n_c^l R_0(\rho^l)}\right]$$

For the energy calculations we need the reciprocal of  $R_0^2(\rho^h)$ :

$$\frac{1}{R_0^2(\rho^h)} = \frac{1}{R_0^2(\rho^l)} + \frac{2 \frac{\partial R_0}{\partial \rho^l} (1 + \rho^l)}{n_c^l R_0^3(\rho^l)}$$

Then the change in bending strain energy for the lamellar phase is

$$n^l S^l \frac{K_c}{2} \frac{2 \frac{\partial R_0}{\partial \rho^l} (1 + \rho^l)}{n_c^l R_0^3(\rho^l)}$$

Since

$$n^l = n_e^l + n_c^l \text{ and } n^l/n_c^l = 1 + \rho^l$$

The differential energy is

$$S^l K_c \frac{\frac{\partial R_0}{\partial \rho^l} (1 + \rho^l)^2}{R_0^3(\rho^l)}$$

**Change in Entropy.** Recall that one can divide  $n$  objects of two distinguishable types of number  $n_e$  and  $n_c$  in  $n!/(n_e!n_c!)$  ways. The number of ways of dividing two independent sets  $n^l$  and  $n^h$  is the product

$$\frac{n^l!}{n_e^l!n_c^l!} \frac{n^h!}{n_e^h!n_c^h!}$$

It is the logarithm of this last quantity that is the entropy of division. We want the difference in this entropy when we make the swap

$$\begin{array}{ll} n_e^l \rightarrow n_e^l + 1 & n_e^h \rightarrow n_e^h - 1 \\ n_c^l \rightarrow n_c^l - 1 & n_c^h \rightarrow n_c^h + 1 \end{array}$$

such that the totals  $n^l = n_e^l + n_c^l$  and  $n^h = n_e^h + n_c^h$  remain fixed. Since the difference in logarithms is the log of the ratio, we want the ratio of the number of ways before and after swapping. After some algebra, this ratio is simply found to be  $\rho^l/\rho^h$ . The relevant entropy change is  $kT \ln(\rho^l/\rho^h)$ . The sum of this entropic term and the bending energy term set to zero gives the relation between  $\rho^h$  and  $\rho^l$  at each point in the lamel-

lar/hexagonal coexistence region:

$$kT \ln \frac{\rho^h}{\rho^l} + S^l K_c \frac{\frac{\partial R_0}{\partial \rho^l} (1 + \rho^l)^2}{R_0^3(\rho^l)} = 0$$

In the special case where  $S$  is fixed, the function

$$\frac{\frac{\partial R_0}{\partial \rho^l} (1 + \rho^l)^2}{R_0^3(\rho^l) \ln \frac{\rho^h}{\rho^l}}$$

is a constant equal to

$$-\frac{kT}{S^l K_c}$$

and one has the relation

$$\frac{kT}{S^l K_c} \ln \rho^h = \frac{\frac{\partial R_0}{\partial \rho^l} (1 + \rho^l)^2}{R_0^3(\rho^l) \ln \rho^l}$$

To compute the number of molecules  $n^h$  in hexagonal phase, one can take the known percent alkane needed to form a particular lipid ratio  $\rho^h$  at zero stress,  $t(\rho^h)$ , and equate  $n^h t(\rho^h)$  to the total amount alkane added to the system.

**Registry No.** DOPE, 2462-63-7; DOPC, 10015-85-7; td, 629-59-4; H<sub>2</sub>O, 7732-18-5.

#### REFERENCES

Belloq, A. M. (1987) Microemulsions: an Overview in *Physics of Complex and Supramolecular Fluids* (Safran, S. A., & Clark, N. A., Eds.) Wiley, New York.

- Bo, L., & Waugh, R. E. (1989) *Biophys. J.* 55, 509-517.
- Duwe, H. P., Englehardt, H., Zilker, A., & Sackmann, E. (1987) *Mol. Cryst. Liq. Cryst.* 152, 1-7.
- Gruner, S. M. (1985) *Proc. Natl. Acad. Sci. U.S.A.* 82, 3665-3669.
- Gruner, S. M. (1989) *J. Phys. Chem.* (submitted for publication).
- Gruner, S. M., Cullis, P. R., Hope, M. J., & Tilcock, C. P. S. (1985) *Annu. Rev. Biophys. Chem.* 14, 211-238.
- Gruner, S. M., Parsegian, V. A., & Rand, R. P. (1986) *Faraday Discuss. Chem. Soc. No. 81*, 29-37.
- Helfrich, W. (1973) *Z. Naturforsch.* 28C, 693-703.
- Kirk, G. L., & Gruner, S. M. (1985) *J. Phys. (Les Ulis, Fr.)* 46, 761-769.
- Luzzati, V. (1968) in *Biological Membranes* (Chapman, D., Ed.) pp 71-123, Academic Press, New York.
- Luzzati, V., & Husson, F. (1962) *J. Cell Biol.* 12, 207-219.
- Parsegian, V. A., Rand, R. P., Fuller, N. L., & Rau, D. C. (1986) *Methods Enzymol.* 127, 400-416.
- Rand, R. P., & Parsegian, V. A. (1989) *Biochim. Biophys. Acta* (in press).
- Rand, R. P., Fuller, N. L., Parsegian, V. A., & Rau, D. C. (1988) *Biochemistry* 27, 7711-7722.
- Schneider, M. B., Jenkins, J. T., & Webb, W. W. (1984) *Biophys. J.* 45, 891-899.
- Schumaster, G., & Sandermann, H. (1976) *Biochim. Biophys. Acta* 448, 642-644.
- Sjolund, M., Rilfors, L., & Lindblom, G. (1989) *Biochemistry* 28, 1323-1329.
- Tate, M. W., & Gruner, S. M. (1987) *Biochemistry* 26, 231-236.
- Tate, M. W., & Gruner, S. M. (1989) *Biochemistry* 28, 4245-4253.
- Turner, D. C., & Gruner, S. M. (1989) *Biophys. J.* 55, 116a.